Genome-wide expression and methylation analyses reveal aberrant cell adhesion signaling in tyrosine kinase inhibitor-resistant CML cells

MEIKE KAEHLER[1], MERIT LITTERST[1], JULIA KOLAROVA[2], RUWEN BÖHM[1],
HENRIKE BRUCKMUELLER[1,3], OLE AMMERPOHL[2], INGOLF CASCORBI[1] and INGA NAGEL[1,4]

[1]Institute of Experimental and Clinical Pharmacology, University Hospital Schleswig-Holstein, Campus Kiel,
D-24105 Kiel; [2]Institute of Human Genetics, Ulm University and Ulm Medical Center, D-89081 Ulm, Germany;
[3]Department of Pharmacy, The Arctic University of Norway, 9037 Tromsø, Norway; [4]Institute of Human Genetics,
University Hospital Schleswig-Holstein, Campus Kiel, D-24105 Kiel, Germany

Abstract. Although chronic myeloid leukemia (CML) can be effectively treated using BCR-ABL1 kinase inhibitors, resistance due to kinase alterations or to BCR-ABL1 independent mechanisms remain a therapeutic challenge. For the latter, the underlying mechanisms are widely discussed; for instance, gene expression changes, epigenetic factors and alternative signaling pathway activation. In the present study, *in vitro*-CML cell models of resistance against the tyrosine kinase inhibitors (TKIs) imatinib (0.5 and 2 μM) and nilotinib (0.1 μM) with biological replicates were generated to identify novel mechanisms of resistance. Subsequently, genome-wide mRNA expression and DNA methylation were analyzed. While mRNA expression patterns differed largely between biological replicates, there was an overlap of 71 genes differentially expressed between cells resistant against imatinib or nilotinib. Moreover, all TKI resistant cell lines demonstrated a slight hypermethylation compared with native cells. In a combined analysis of 151 genes differentially expressed in the biological replicates of imatinib resistance, cell adhesion signaling, in particular the cellular matrix protein fibronectin 1 (FN1), was significantly dysregulated. This gene was also downregulated in nilotinib resistance. Further analyses showed significant FN1-downregulation in imatinib resistance on mRNA (P<0.001) and protein level (P<0.001). SiRNA-mediated FN1-knockdown in native cells reduced cell adhesion (P=0.02), decreased imatinib susceptibility visible by higher Ki-67 expression (1.5-fold, P=0.04) and increased cell number (1.5-fold, P=0.03). Vice versa, recovery of FN1-expression in imatinib resistant cells was sufficient to partially restore the response to imatinib. Overall, these results suggested a role of cell adhesion signaling and fibronectin 1 in TKI resistant CML and a potential target for novel strategies in treatment of resistant CML.

Introduction

The myeloproliferative syndrome chronic myeloid leukemia (CML) is predominantly caused by reciprocal translocation t(9;22)(q34;q11) with subsequent formation of the *BCR-ABL1* fusion gene resulting in malignant cell transformation (1,2). Since the development of tyrosine kinase inhibitors (TKIs), CML can be effectively treated by blocking the BCR-ABL1 kinase domain (3,4). This treatment is tremendously successful in clinical routine showing 83.3% 10-year survival rates, which are comparable to healthy individuals (5). However, besides primary resistance, 20 to 25% of TKI-treated CML patients acquire therapy resistance after initial cytogenetic or molecular remission (5,6). Only some of these patients can be helped with second or third generation TKIs (for example, nilotinib, dasatinib or ponatinib) (4,7) dependent on the underlying mechanisms of TKI resistance, which is unknown in numerous cases.

In ~60% of all clinical cases, resistance occurs due to gene amplification/overexpression or point mutations in the BCR-ABL1-kinase, i.e. Y253H, E255V, T315I, F317L and F359V (8,9). For the remaining cases, various BCR-ABL1-independent mechanisms are discussed; for instance, upregulation of efflux transporters of the ABC-binding cassette family, alternate activation of signaling pathways and adaptions of the DNA methylation profile or dysregulation of microRNA expression (10-13). Further, persistence of cancer stem cells may contribute to resistance (14-16).

In the present study, global transcriptional and epigenetic changes in different *in vitro*-TKI resistance cell models of imatinib and nilotinib were investigated. Recurrent

Correspondence to: Professor Ingolf Cascorbi, Institute of Experimental and Clinical Pharmacology, University Hospital Schleswig-Holstein, Campus Kiel, 3 Arnold-Heller Street, D-24105 Kiel, Germany
E-mail: cascorbi@pharmakologie.uni-kiel.de

genome-wide expression and DNA methylation profiles were obtained from biological replicates derived from chronic exposure to low and high concentrations of imatinib, as well as to nilotinib to analyze whether there are similarities of gene expression changes caused during development of TKI resistance. Based on these findings, aberrant cell adhesion signaling was identified to be recurrently differentially dysregulated in imatinib and nilotinib resistance. Thus, the role of fibronectin 1 (FN1) in imatinib resistance was analyzed providing insights into the mechanisms underlying TKI resistance.

Materials and methods

Reagents, cell lines and generation of resistant cells. K-562 cells (RRID: CVCL_0004), established from the pleural effusion of a 53-year old woman (Lozzio and Lozzio, 1975), were obtained from the German Collection of Microorganisms and Cell Cultures (DSMZ). The cells were maintained and imatinib resistant cell lines were obtained as previously described in two independent biological replicates for each subline (11,17). Briefly, native cells were exposed initially to low TKI concentration until the cells were resistant to this concentration as the cellular proliferation rate was restored. After 10-14 d, the TKI concentration was slowly increased. This was repeated until the desired concentrations of 0.5 μM or 2 μM imatinib and 0.1 μM nilotinib were reached. Imatinib and nilotinib were obtained from Novartis International AG and stored at -20˚C in 10 mM aqueous stock solutions. Both TKIs were diluted to 100 μM working solutions in RPMI-1640 (Gibco; Thermo Fisher Scientific, Inc.). Authenticity of TKI resistant K-562 cell lines was confirmed by short tandem repeat analysis using GenePrint 10 System (Promega Corporation). *BCR-ABL1* mutations were analyzed as previously described (17). None of the sublines showed mutations in *BCR-ABL1*. For inhibition assays, 1x10^6 cells were incubated with 10 μM FAK14 inhibitor (Sigma-Aldrich; Merck KGaA) or 50 μM ATN-161 (Bio-Techne) for 24 h.

RNA and DNA extraction. Total RNA was isolated using miRVana microRNA isolation kit (Thermo Fisher Scientific, Inc.) or PeqGOLD TriFast (VWR International, LLC) according to the manufacturer's recommendation. Cell line DNA was purified using Gentra Puregene kit (Qiagen GmbH) according to the manufacturer's protocol.

Genome-wide expression analysis. Genome-wide expression analyses of two biological and four technical replicates of native, imatinib and nilotinib resistant K-562 sublines (native; lowIM: 0.5 μM imatinib resistant; highIM: 2 μM imatinib resistant; N: 0.1 μM nilotinib resistant) was performed using HuGene 2.0 ST arrays (Affymetrix; Thermo Fisher Scientific, Inc.) and 100 ng RNA of each sample according to the manufacturer's recommendations. Data were analyzed with Transcriptome Analyses Console (Thermo Fisher Scientific, Inc.) and genes with fold changes ±2 and false discovery rate (FDR) corrected P-value P<0.05 were considered to be differentially expressed. Subsequent analyses were performed using Venn diagrams [(18); PNNL, omics.pnl.gov], Cluster 3.0 software (Stanford University, USA), KEGG pathway

prediction using DAVID Functional Annotation Tool (DAVID Bioinformatics Resources 6.8), STRING database (string-db. org, Version 11.5 with medium confidence), as well as R 4.0.3. with the 'GOplot' package (19,20).

Genome-wide methylation analysis. Methylation analyses of native and TKI resistant cell lines were performed using Infinium MethylationEPIC BeadChip (Illumina, Inc.) for 250 ng DNA of each sample (native, lowIM, highIM, N) according to the manufacturer's recommendation. Data were analyzed using Genome Studio Software (Illumina, Inc.) with 1% FDR and calculation of delta beta values $\Delta\beta$ with P-value FDR correction. CpGs with $\Delta\beta \geq 0.2$ and $P_{adj}<0.05$ were considered to be differential methylated. Genes were chosen for subsequent analyses with at least three differentially methylated CpGs/gene and clustered according to their genomic location. Principle component analysis (PCA) was performed using Python 3.7.1 (21) with the packages skleran 0.20.1, pandas 0.23.44 and numpy 1.19.3, frequency scatter plots using R. Statistical analyses were performed with GraphPad Prism (Version 8.0 for Windows; GraphPad Software, Inc.).

Reverse transcription-quantitative (RT-q) PCR. Total RNA (1 μg) was reversely transcribed using random hexamer primers and the High Capacity cDNA Synthesis kit (Thermo Fisher Scientific, Inc.) according to the manufacturer's protocol. RT-qPCR of target genes was performed in triplicates on the QuantStudio 7 device (Thermo Fisher Scientific, Inc.) with the assays *BCL-2* (Hs00608023_m1), *DNASE2* (Hs00172391_m1), *FN1* (Hs01549976_m1), *IFI30* (Hs00173838_m1), *NMU* (Hs00183624_m1), *PDE4DIP* (Hs00206200_m1), *TBP* (Hs00427620_m1) and *GAPDH* (Hs02786624_g1) serving as internal controls. Universal Master Mix II, without UNG, (Thermo Fisher Scientific, Inc.) using default cycling conditions, was used for qPCR. Statistical analysis was performed as previously described (22).

Whole cell lysates and immunoblotting. Whole cell lysates and immunoblotting were performed as previously described (17,23,24). For membrane fractionation, the Plasma Membrane Protein Extraction kit (Abcam) was used. A total of 20 μg of protein was loaded onto the respective membranes and blots were probed with antibodies obtained from Cell Signaling Technology, Inc. [(p-ERK: cat. no. 9102; RRID: AB_330744; 1:2,000), (p-NFκB: cat. no. 93H1; RRID: AB_10827881; 1:1,000) NFκB: cat. no. D14E12; RRID: AB_10859369; 1:1,000) p-p38: cat. no. 9211, RRID: AB_331641; 1:500)], Santa Cruz Biotechnology, Inc. [(ERK: cat. no. sc-514302; RRID: AB_2571739; 1:750; FN1: cat. no. sc-8422; RRID: AB_627598; 1:200), GAPDH: cat. no. sc-47724; RRID: AB_627678; 1:1,000), (p38: cat. no. sc-7972; RRID: AB_628079; 1:1,000)] or LI-COR Biosciences [(anti-mouse: cat. no. 926-32210; RRID: AB_621842; cat. no. 926-680707; RRID: AB_10956588), anti-rabbit: cat. no. 926-68071; RRID: AB_10956166; cat. no. 926-32211; RRID: AB_621843; all 1:10,000]. Primary antibodies were diluted in Intercept/TBS blocking solution (LI-COR Biosciences) supplemented with 0.2% Tween-20, secondary antibodies were diluted in TBS supplemented with 0.1% Tween-20.

Cell adhesion assay. Corning Matrigel basement membrane mix (VWR) was thawed overnight at 4°C. A total of 50 μl/well were added onto dark 96-well plates under pre-chilled conditions. After 1 h consolidation, the plate was washed with pre-warmed serum-free media and dried for 30 min. The cell adhesion assay was performed using Vybrant Cell Adhesion Assay kit (Thermo Fisher Scientific, Inc.) according to the manufacturer's protocol. Briefly, 1.5×10^6 cells were used for each sample, washed twice with pre-warmed PBS and resuspended in serum-free media. A total of 5 μM calcein AM was added and incubated for 30 min at 37°C and 5% CO_2. After washing twice with pre-warmed PBS and resuspension in serum-free RPMI-1640, 100 μl cell suspension was added to the pre-coated plate and incubated for 90 min at 37°C, 5% CO_2. Wells were washed twice with pre-warmed PBS to remove non-adherent cells. After addition of 200 μl PBS, the plates were measured using 494 nm as absorbance and 517 nm as emission wavelength at an Infinite M200 Pro device (Tecan Group, Ltd.).

Cloning. *FN1* coding plasmids (Gene ID: 2335, ABIN3996197, antibodies-online) were subcloned into the pSelect-puromycin-mcs vector (Sigma-Aldrich; Merck KGaA) using the Pfu-X Core kit (Jena Bioscience) using the following set of primers: FN1_pSELECT_forward, 5'-GCGTGTCGACGG ATCATGCTTAGGGGTCCGGGG-3' and reverse, 5'-GCC AGCTAGCCCATGTTACTCTCGGGAATCTTCTCTGTC-3' with annealing at 61°C, the restriction enzymes *BamHI* and *NcoI* (New England BioLabs, Inc.), cloning enhancer and the In-Fusion HD kit (Takara Bio Europe SAS).

Plasmid and siRNA transfection. Cells (2×10^6) were transfected with 5 μg of the respective plasmid (pSELECT-empty; pSELECT-FN1) using nucleofection and the nucleofector 2 b device (Lonza Group Ltd.). After 1 h of transfection, imatinib-resistant cells were seeded onto respective cell culture plates to analyze cellular fitness followed by 48 h exposure to 0.5 μM imatinib or used for expression analyses as previously described (17,22). For siRNA transfection, K-562 cells were transfected with 100 nM Silencer Select Negative Control #1 siRNA (cat. no. 4390843) or Silencer Pre-designed siRNA 10826 (sense: 5'-GGCUCAGCAAAU GGUUCAGtt-3', antisense: 5'-CUGAACCAUUUGCUG AGCCtg-3'; AM16708; Thermo Fisher Scientific, Inc.) as aforementioned. After 24 h of transfection, cells were seeded onto respective cell culture plates and exposed to 2 μM imatinib for 48 h or transferred for RNA isolation. In case of proliferation analyses, cells were incubated for 24 h with 2 μM imatinib.

Cellular fitness assays. Cell numbers were obtained by trypan blue staining as previously described (22). WST-1 (Sigma-Aldrich; Merck KGaA) and Caspase Glo 9 Assay (Promega Corporation) were performed as previously described (17). Proliferation was analyzed by Ki-67 expression using human MKI67 ELISA kit (cat. no. MBS8291369, MyBioSource, Inc.) according to the manufacturer's recommendation with 50 μg protein/well. Data were analyzed normalizing IM-treated to non-treated samples followed by statistical analyses as described below.

Software & statistical analysis. Primers were designed using the InFusion Cloning primer design tool (Takara Bio Europe SAS). Densitometry was performed using Empiria Studio 1.2 (LI-COR Biosciences). Spearman-Rank correlation was calculated using Cluster 3.0 (Stanford University, Stanford, CA, USA). Unless not otherwise described, statistical analysis was performed using one-way ANOVA with subsequent Dunnett's test, unpaired Student's or Welch's t-test and the GraphPad prism software (Version 8.0; GraphPad Software, Inc.). $P < 0.05$ was considered to indicate a statistically significant difference.

Results

Gene expression changes between the biological replicates of TKI resistant CML cells. To study mechanisms of TKI resistance in CML cells, an *in vitro*-TKI CML cell line model of CML cells being resistant to low (lowIM: 0.5 μM) and high (highIM: 2 μM) concentrations of imatinib or to 0.1 μM nilotinib (N, Fig. 1A) was generated. At lowIM, the number of differentially expressed genes were 1,286 and 1,287 in the biological replicates, respectively (Fig. 1B-D), and there was an overlap of 636 unidirectional differentially expressed genes with 67% being downregulated (Fig. S1). At highIM, a total of 1,073 and 1,267 genes were differentially expressed in the biological replicates. A total of 317 genes were unidirectionally expressed in both replicates with 35% being downregulated indicating larger differences (Figs. 1B-D and S1). The difference was even more profound in 0.1 μM nilotinib resistance: 1,898 and 1,083 genes were differentially expressed in the biological replicates with 469 unidirectional differentially expressed genes among them 25% downregulated genes (Fig. 1B-D and S1). Overall, the differences in gene expression were more pronounced in CML cells resistant to higher imatinib concentrations or nilotinib.

Recurrent expression changes and pathway analysis of imatinib and nilotinib resistance. The extent of gene expression changes among imatinib resistant CML cells differed with respect to imatinib concentration, but also between the biological replicates. In replicate 1, there was a total of 270 genes that were differentially expressed in lowIM, as well as highIM concentrations compared with native CML cells. By contrast, in replicate 2, a total of 691 genes was significantly altered in both, lowIM and highIM resistant sublines compared with their native progenitor cells (Fig. 2A). Genes being differentially expressed in both replicates in both imatinib concentrations were considered as most promising to be associated with drug resistance. There were 151 unidirectional differentially expressed genes, 67 among them were upregulated and 84 downregulated in resistant cell lines compared with native cells (Fig. 2B). For these genes, pathway prediction was performed disclosing an enrichment in signaling pathways and malignant signaling transduction in cancer (R1: P_{adj}=0.05, R2: P_{adj}=0.04). Further, genes involved in focal adhesion pathways were found to be enriched in the biological replicates of imatinib resistant sublines compared with TKI native cells (P_{adj}=0.01), among them B-cell lymphoma 2 (*BCL-2*), insulin-like growth factor 1 (*IGF1*), reelin (*RELN*) and fibronectin 1 (*FN1*) (Fig. 2C, Table SI). For nilotinib resistance, no significant enrichment of pathways was detected for the overlap of the two biological
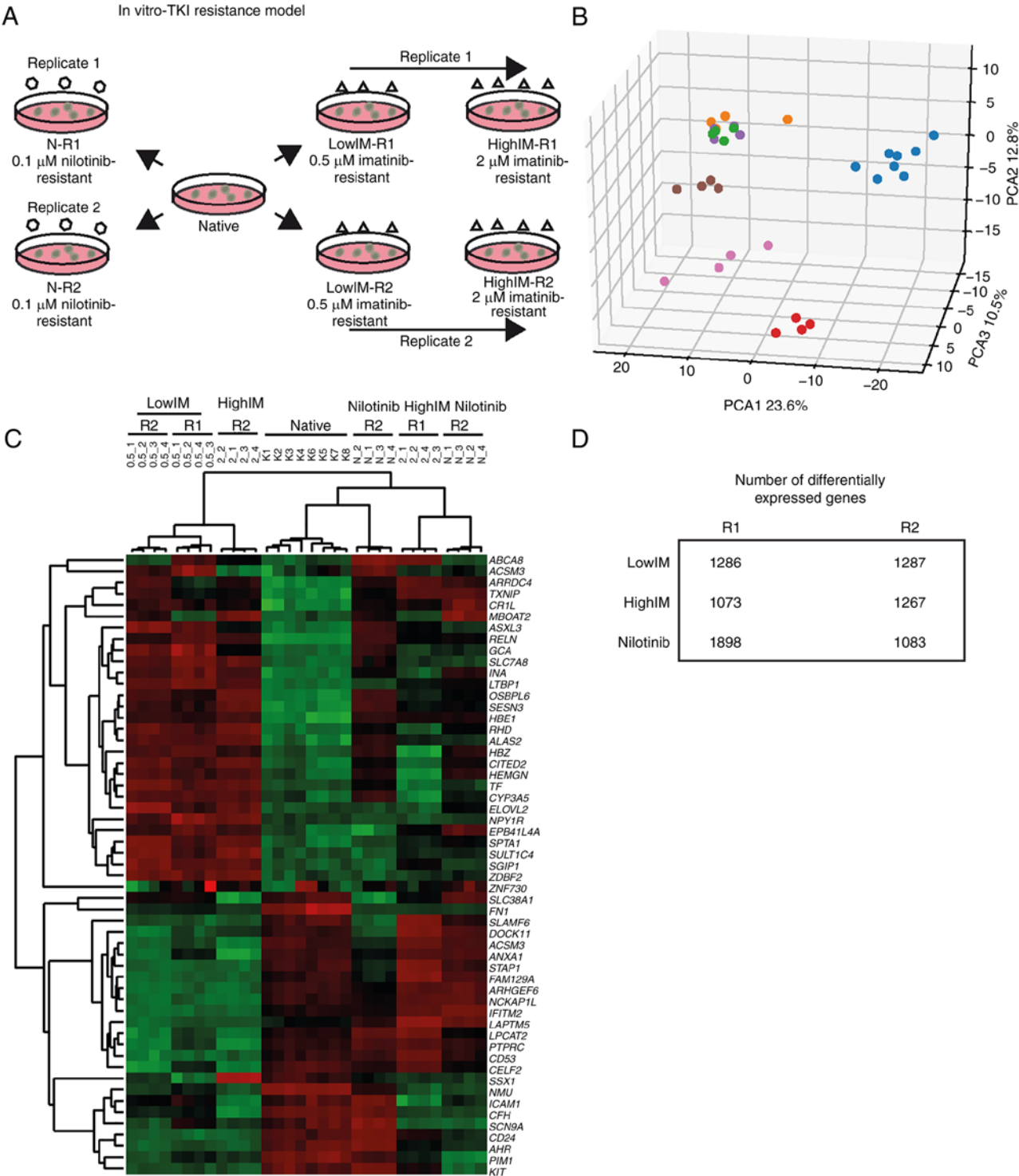
Figure 1. Array-based gene expression profiles of TKI resistant CML cells compared with native counterparts. (A) Schematic representation of the *in vitro*-TKI resistance model used for the present study. (B) PCA of TKI resistant cell lines. Blue: native cells; orange: lowIM-R1; green: lowIM-R2; red: highIM-R1; purple: highIM-R2; brown: N-R1; pink: N-R2. (C) Heatmap of Spearman-Rank-correlation of z-transformed differentially expressed gene expression levels in TKI resistance with fold change ± 5 and $P_{adj} < 0.05$. Red: high expression; green: low expression level. (D) Number of differentially expressed genes in TKI resistance with fold change ± 2 and $P_{adj} < 0.05$. TKI, tyrosine kinase inhibitor; CML, chronic myeloid leukemia; PCA, Principle component analysis; lowIM, 0.5 μM imatinib resistant; highIM, 2 μM imatinib resistant; N, 0.1 μM nilotinib resistant; R1, resistant subline 1; R2, resistant subline 2.

replicates. When comparing gene expression of all replicates of imatinib and nilotinib resistance, there was an overlap of 71 genes concomitantly dysregulated (Fig. S2). For these genes, the pathway prediction analysis revealed no enrichment. However, STRING analysis showed a network involving *FN1*, serglycin (*SRGN*) and *IGF1* with the highest downregulation

for *FN1* in all TKI resistant sublines (fold change: highIM -11.24, N -11.95, Fig. S2).

Methylation alterations in imatinib and nilotinib resistance. Genome-wide methylation analyses were performed to compare alterations during the development of TKI
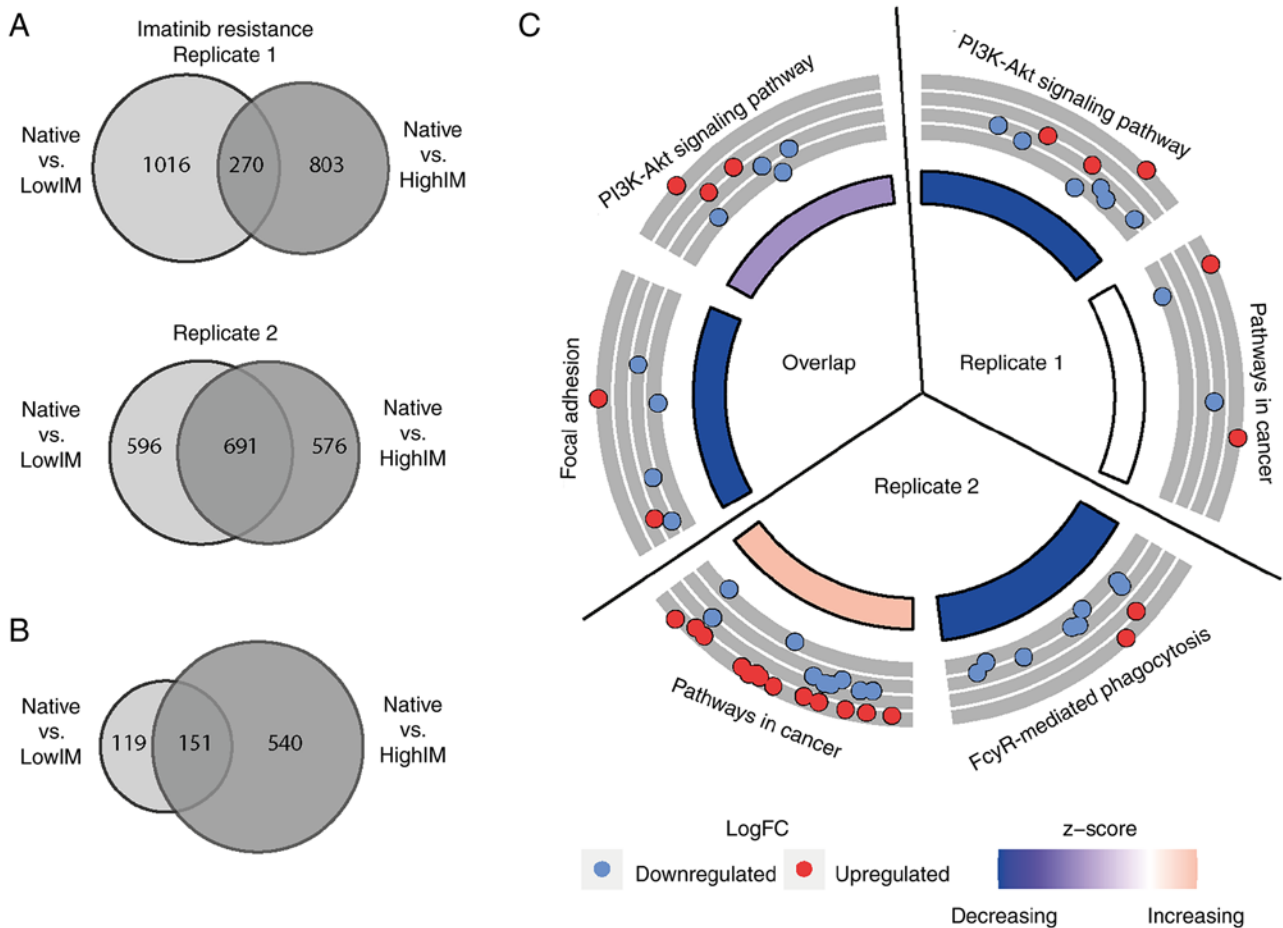
Figure 2. Differential gene expression in biological replicates of imatinib resistance. (A) Venn diagrams of differentially expressed genes in each subline and (B) in the overlap of both replicates of imatinib resistance compared with native K-562. Numbers indicate differentially expressed genes comparing native cells to lowIM and highIM. (C) GoPlot of significantly enriched KEGG pathways with differentially expressed genes in imatinib resistance shown for replicate 1, replicate 2 of imatinib resistance, as well as the combined analysis of both replicates (overlap) displaying the gene expression fold changes (logFC) and the z-score of the pathway prediction to indicate the direction of the overall changes. lowIM: 0.5 μM imatinib resistant; highIM: 2 μM imatinib resistant; R1: resistant subline 1; R2: resistant subline 2.

resistance of imatinib and nilotinib resistant sublines. Overall, genome-wide methylation profiles displayed a pattern similar to the gene expression profiles as revealed by the respective PCA (Fig. 3A). In imatinib resistant sublines, 6.6 to 11.2% of CpGs were differentially methylated, while 5.0 to 9.5% of CpGs were differentially methylated in nilotinib resistance (Fig. 3B). Applying a filter of ≥3 concurrently altered CpGs per gene, 4.0 to 7.5% CpGs were differentially methylated in imatinib resistance. Of note, large differences were observed in nilotinib resistance with 6.0% in N-R1 and 2.7% in N-R2 (Fig. 3B).

Next, mean DNA methylation of the TKI resistant sublines was analyzed taking into account the genomic localization. An increase in overall DNA methylation (in all genomic regions), as well as in transcriptional start side (TSS), gene body and enhancer region methylation were observed in all resistant sublines compared with native K-562 cells (Fig. 3C). Regarding the distribution of differentially methylated CpGs in the genome, hardly any difference was detected between TKI resistant sublines (Fig. 3D). The increase in methylation in all genomic regions was also visible in the frequency distribution of each TKI resistant subline showing a hypermethylation particularly in highIM, but less pronounced in lowIM and

nilotinib (Fig. 3E). These findings suggested moderate methylation changes in the TKI resistant cell lines compared with their native counterparts.

Association of DNA methylation and gene expression in TKI resistance. In an analysis of genes that were both differentially expressed and differentially methylated, and thereby potentially altered by methylation, 50 genes were detected in all biological replicate of imatinib resistance (Table SII). In nilotinib resistance, large differences between the replicates were observed with 95 genes in N-R1 and 21 in N-R2. The overlap of genes being differentially methylated and expressed between the biological replicates was 12 in lowIM, 17 in highIM and 7 for nilotinib resistant cells (Table SIII). Filtering for differentially expressed genes with differentially methylated CpGs in the TSS region of the respective genes in all biological replicates, only 5 genes, namely *BCL-2*, *PDE4DIP*, *NMU*, *IFI30* and *DNASE2* were detected (Table SIII). For four of these five genes (*DNASE2*, *IFI30*, *NMU* and *PDE4DIP*), mRNA-downregulation in lowIM and highIM was confirmed by RT-qPCR (Fig. S3). This suggested that consistent methylation changes during development of TKI resistance are limited to distinct genes.
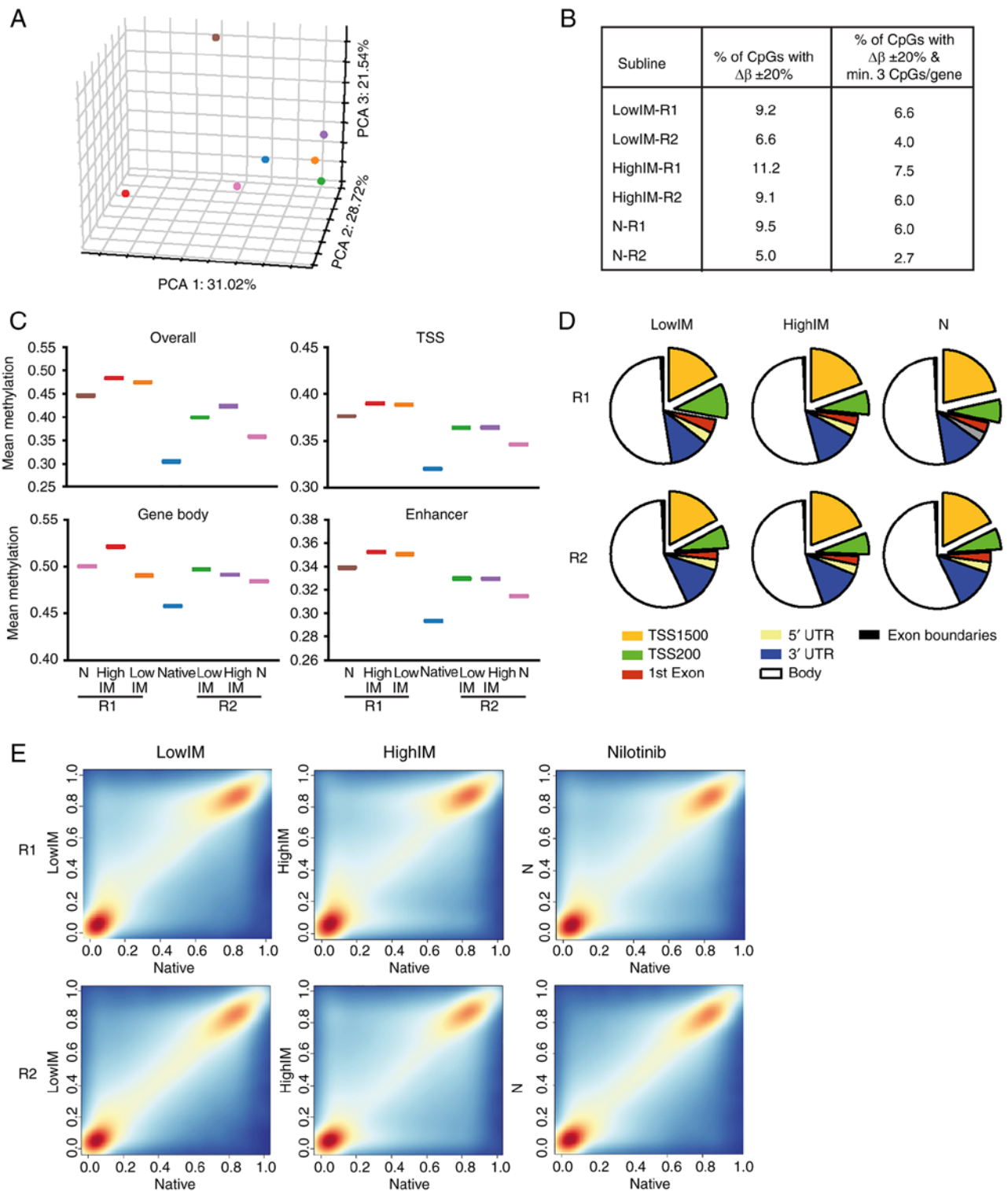
Figure 3. Genome-wide methylation profile of TKI resistance. (A) PCA of TKI resistant sublines. Blue: native cells; orange: lowIM-R1; green: lowIM-R2; red: highIM-R1; purple: highIM-R2; brown: N-R1; pink: N-R2. (B) Percentage of differentially methylated CpGs in TKI resistant sublines compared with native K-562 with $\Delta\beta \pm 20$ % and $P_{adj}<0.05$ and filtered for minimum 3 CpGs per gene. (C) Mean methylation of TKI resistant cell lines depicted for overall, TSS, gene body and enhancer methylation. (D) Distribution of differentially methylated CpGs in genomic regions in each subline of TKI resistance. (E) Frequency scatter plots of differentially methylated CpGs in all genomic regions of each TKI resistant subline. Red: hypermethylation; blue: hypomethylation. TKI, tyrosine kinase inhibitor; TSS, transcription start site; lowIM, 0.5 μM imatinib resistant; highIM, 2 μM imatinib resistant; N, 0.1 μM nilotinib resistant; R1, resistant subline 1; R2, resistant subline 2; PCA, principle component analysis.

Aberrant cell adhesion signaling reveals fibronectin 1 as modulator of imatinib resistance. The gene expression profiles of imatinib resistant cell lines pointed to dysregulation of cell adhesion signaling indicated by pathway enrichment in focal adhesion and PI3K-Akt-signaling. Among the differentially expressed genes, expression of the extracellular matrix protein FN1 was most substantially reduced in imatinib resistance compared with native cells (mean fold change:
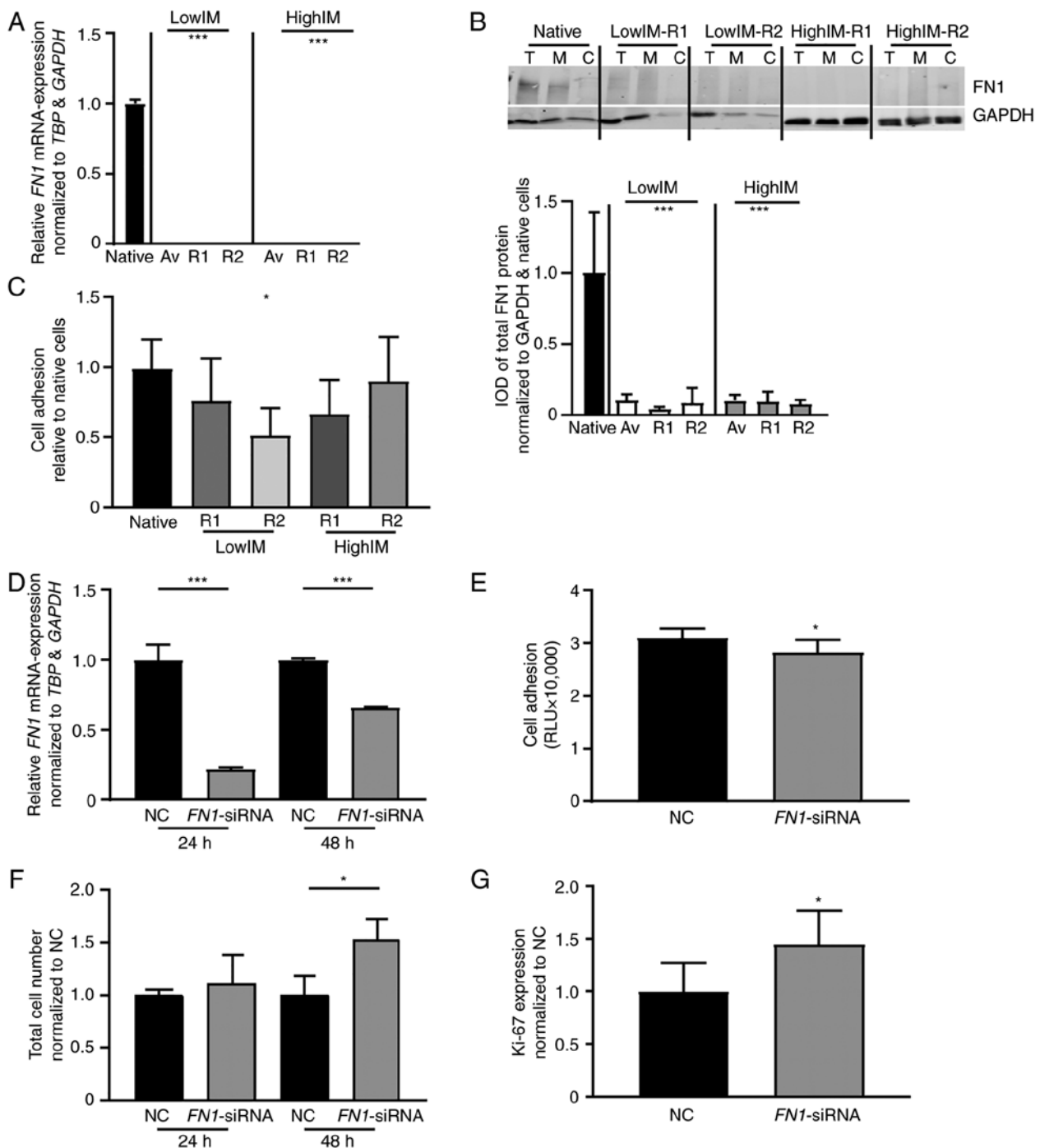
Figure 4. *FN1* expression and siRNA-mediated knockdown in CML cells. (A-C) *FN1* expression in IM-resistant sublines. (A) mRNA expression of *FN1* in IM-resistant sublines compared with *TBP*, *GAPDH* and relative to native cells. (B) Immunoblotting against FN1 in IM-resistant sublines (top panel) followed by densitometric analyses (lower panel) compared with GAPDH. Av, Average/mean expression; T, Total protein; M, Membrane fraction; C, Cytosolic fraction. (C) Cell adhesion capacity of IM-resistant K-562 cells to Matrigel coated surfaces normalized to native cells. (D-G) siRNA-mediated knockdown of *FN1* in K-562 cells. (D) *FN1*-mRNA expression 24 and 48 h after siRNA-transfection analyzed by reverse transcription-quantitative PCR and normalized to *TBP*, *GAPDH* and NC. (E) Cell adhesion capacity of K-562 cells after siRNA-transfection. (F) Total cell number measured by trypan blue staining and (G) Ki-67 expression after siRNA-transfection of K-562 cells after exposure to 2 μM IM and normalized to NC. N=3; *P<0.05 and ***P<0.001. FN1, matrix protein fibronectin 1; CML, chronic myeloid leukemia; lowIM, 0.5 μM imatinib resistant; highIM, 2 μM imatinib resistant; R1, resistant subline 1; R2, resistant subline 2; IM, imatinib; IOD, integrated optical density; NC, negative control transfection; RLU, relative luminescence units; siRNA, small interfering RNA.

-9.8, P_{adj}=9.5x10^{-15}). This gene was also considerably downregulated in both replicates of nilotinib resistance (mean fold change: -11.9, P_{adj}=1.8x10^{-7}). FN1 dysregulation was confirmed by comparing native K-562 with lowIM and highIM cells on mRNA and protein level, respectively. *FN1* mRNA was significantly decreased in all tested imatinib resistant sublines compared with native cells (lowIM: P<0.001, highIM: P<0.001; Fig. 4A). A similar result was obtained on protein level, as FN1 showed lower abundance in all imatinib resistant cell lines compared with native cells (lowIM: P<0.001, highIM: P<0.001; Fig. 4B). In a next step, cell adhesion capacity of imatinib resistant cell lines was analyzed investigating the

binding to Matrigel-coated plates and compared with the binding capacity of native K-562 cells. A significantly reduced cell adhesion capacity was only detected in lowIM-R2 (P=0.02; Fig. 4C).

Next, siRNA-mediated knockdown of *FN1* expression was performed in native K-562 cells. Transfection of a *FN1*-specific siRNA led to a significant reduction of *FN1*-expression after 24 (P<0.001) and 48 h (P<0.001), accompanied by reduced cell adhesion to Matrigel (P=0.02; Fig. 4D and E). Moreover, under exposure to 2 μM imatinib, *FN1*-knockdown resulted in a 1.5-fold higher cell number after 48 h (P=0.03), as well as a 1.45-fold higher Ki-67 expression (P=0.04; Fig. 4F and G). This indicated a decreased imatinib susceptibility after knockdown of *FN1*.

Vice versa, lowIM cells were transfected with an *FN1*-encoding expression plasmid. Overexpression of *FN1* in lowIM-R1 (P<0.001) and lowIM-R2 (P=0.002, Fig. 5A) led to increased cell adhesion to Matrigel (lowIM-R1: 19.9 %, P=0.03; lowIM-R2: 11.3%, P=0.04; Fig. 5B). Moreover, after restoration of *FN1*-expression, imatinib resistant sublines showed reduced cell numbers (lowIM-R1: -26.5%, P=0.008; lowIM-R2: -23.4 %, P=0.04; Fig. 5C), cell viability (lowIM-R1: -38.7%, P=0.003; lowIM-R2: -33.7%, P=0.004; Fig. 5D), as well as proliferation rates in both tested cell lines (lowIM-R1: -49.3%, P<0.001; lowIM-R2: P=0.04; Fig. 5E) compared with respective sublines without *FN1* overexpression. These data indicated that FN1 affects the response to imatinib in CML cells.

As FN1 is known to activate integrin α5β1, which leads to intracellular signaling via the focal adhesion kinase (FAK) and subsequently alteration of survival and proliferation signaling via MAP kinase, p38 and NFκB pathways, lowIM-R1 cells were transfected with FN1 and effects on the intracellular signaling cascade were analyzed. Restoration of FN1 expression led to a significant decrease in p38- (-0.50, P=0.04) and ERK-phosphorylation (-0.36, P=0.04), but not of NFκB (Fig. 5F). Inhibition of integrin α5β1 by ATN-161 in lowIM-R1 cells led to a reduction of ERK-phosphorylation (-0.40, P=0.04), while FAK inhibition using FAK14 led to a decrease in p-p38 (-0.87, P=0.002), p-ERK (-0.72, P<0.001) and p-NFκB (-0,76, P=0.01). These findings stand in line with the observed reduction in total cell number and proliferation rate after FN1-transfection (Fig. 5F).

Discussion

Using an *in vitro*-CML cell line model of drug resistance against imatinib and nilotinib, drug concentration-dependent differences were detected in overall gene expression and DNA methylation. Differential expression of genes associated with cell adhesion signaling, particularly *FN1*, was observed as a common phenomenon in all imatinib resistant, but also nilotinib resistant sublines. FN1 was proven to improve imatinib susceptibility by transfection experiments.

In the present study, gene expression profiles of treatment-naïve and TKI resistant cell lines were obtained using microarrays. These arrays are a well-established system to analyze gene expression, biomarker identification or genotyping (25,26). Although next generation sequencing has several benefits, such as being a flexible, open, but also

cost-intensive system for a high coverage, microarrays still provide a useful tool for expression analyses of low expressed genes, thereby being a closed system with only a limited straightforward bioinformatic pipeline (26). The HuGene 2.0 ST arrays (as well as their successor Clariom D) from Affymetrix/Thermo Fisher Scientific, Inc. are well known to have a high reproducibility of >0.9 (27-29). However, to cope with experimental validation, 4 technical replicates for each cell line were included into our analyses. These replicates showed a high reproducibility, as visible in the PCA, but also in the number of dysregulated genes leading to the assumption that the observed differences in the gene expression profiles are indeed due to differences in the resistant cell lines and not due to methodological problems. In the gene expression profiles, there were relatively large differences between the replicates of cells being resistant to high concentrations of imatinib or to nilotinib, but less differences were observed in cells being resistant to low imatinib concentrations. This gives hint to dose-dependent mechanisms of resistance standing in line with previous studies (30,31). Only few similarities of differentially expressed genes could be detected between the two TKIs indicating distinct mechanisms of resistance against TKIs. A similar phenomenon was described in a study from Kim *et al* (31), in a comparison of nilotinib to imatinib resistant cells showing profound differences in the expression profile of TKI resistant sublines and only a small overlap. In the present study, recurrent differential expression of genes associated with PI3K-Akt signaling and focal adhesion was observed in all imatinib resistant sublines compared with native K-562 cells. In a previous study from Chung *et al* (30), overexpression of genes associated with transcription or apoptosis was determined, as well as downregulation of protein and energy metabolism. As signaling transduction was significantly altered in our model, this only partially stands in line with the present findings. Regarding the observed gene expression changes associated with cell adhesion signaling in imatinib resistance, this was also detected by Kim *et al* (31) showing upregulation of genes associated with cell adhesion in TKI resistant cells.

In several studies, it was shown that cell adhesion plays an important role in leukemia, as it affects the interaction of tumor cells with the bone marrow microenvironment or stroma (32). In addition, hyperactivation of the tyrosine kinase BCR-ABL1 was shown to change the leukemic phenotype, as well as the activation state of cell adhesion molecules, for example beta-1 integrins (33-36). In the present study, a downregulation of FN1 in imatinib resistant cells was observed compared with their native counterparts. In several *in vitro*-studies, it was shown that adhesion to extracellular matrix proteins, for example FN1, promotes apoptotic resistance under TKI treatment and the binding is influenced by these drugs contributing to the term 'cell adhesion-mediated drug resistance' (37,38). These studies were performed using treatment-naïve cells analyzing the drug response and not cells with a persistent resistance. In both studies, FN1 was used to coat surfaces and measure cell adhesion. However, in the present study, FN1-transfection experiments were performed to directly analyze its role in TKI resistance demonstrating that FN1 itself influences the response to TKIs. This revealed that binding to FN1 protects the cells to initial exposure of treatment-naïve cells to imatinib, while
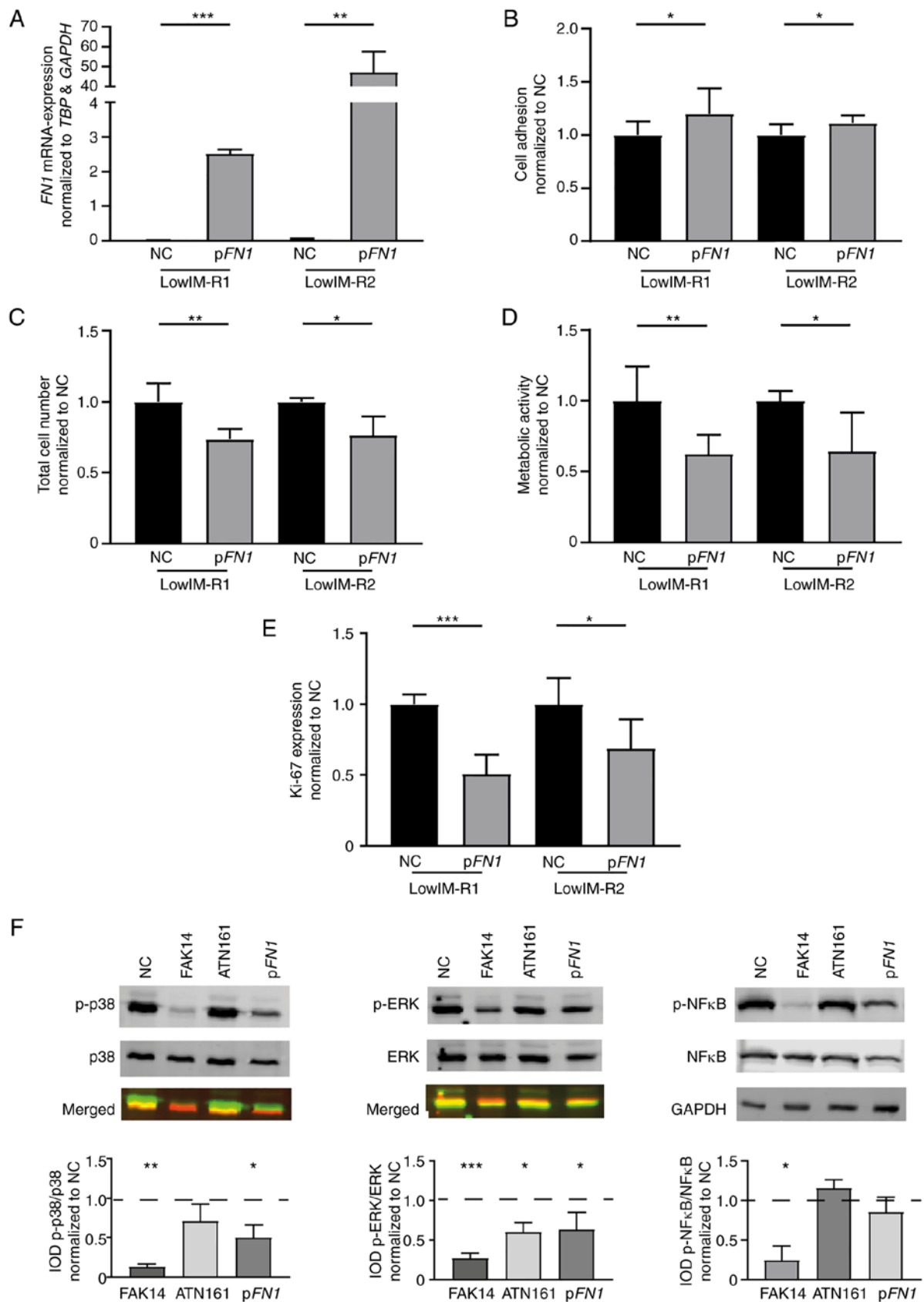
Figure 5. Restoration of *FN1* expression in imatinib resistant cell lines. LowIM-R1 and lowIM-R2 were transfected with an *FN1*-encoding plasmid with subsequent analyses of cellular fitness. (A) *FN1* mRNA expression after plasmid transfection analyzed by reverse transcription-quantitative PCR and normalized to *TBP* and *GAPDH*. (B) Cell adhesion to a Matrigel-coated surface after plasmid transfection and normalized to NC. (C) Total cell number measured by trypan blue staining, (D) Metabolic activity analyzed by respiratory chain function and (E) Ki-67 expression of *FN1*-transfected sublines after exposure to 0.5 μM IM normalized to NC. (F) Phosphorylation of p38 (left), ERK (middle) and NFκB (right) after restoration of FN1-expression in lowIM-R1 cells compared with inhibition of the focal adhesion kinase using FAK14 or integrin α5β1 by ATN161 followed by densitometric analysis. GAPDH is shown as housekeeper. N=3; *P<0.05, **P<0.01 and ***P<0.001. FN1, matrix protein fibronectin 1; IM, imatinib: NC, negative control transfection/empty vector control; p*FN1*, plasmid encoding *FN1*; lowIM-R1, 0.5 μM imatinib resistant cells replicate 1; lowIM-R2, 0.5 μM imatinib resistant cells replicate 2.

in the present study, it was also possible to restore imatinib susceptibility of already resistant cells by FN1 transfection. Therefore, it appears that not only the binding to extracellular FN1 modulates drug resistance, but the production of FN1 by the cell itself can influence drug response and resistance. These findings suggested that FN1 does not only play a role as adhesion molecule, but also impairs TKI resistance. In a study from Kumar *et al* (39), it was demonstrated that TKI resistance mediated by the BCR-ABL1 gatekeeper mutation T315I alters cell adhesion and niche localization compared wild-type BCR-ABL1 by increased expression of integrin β3 and integrin-like kinase (ILK). Thereby the deposition of FN1 was decreased promoting malignant progression. In addition, it was identified that treatment of BCR-ABL^{T315I} CML with FN1 or an ILK inhibitor significantly increases survival of mice in a xenograft model (39). It was observed that FN1 knockdown indeed enhanced imatinib resistance, while restoration of FN1 expression in imatinib resistant sublines re-established imatinib sensitivity. These findings stand in line with the observed inhibition of proliferation after FN1 treatment of BCR-ABL^{T315I}, but also B-ALL cells (39,40). However, significant dysregulation of either integrin β3 or ILK in the gene expression profiles of our *in vitro*-model was not observed. After restoration of FN1-expression in imatinib resistant cells, a decrease of p38 and ERK-phosphorylation was observed pointing to an involvement of these pathways to the detected decreased proliferation and cell numbers after FN1 transfection. While the effect was less pronounced for FN1 compared with FAK inhibition, the absence of effects after integrin α5β1 inhibition revealed that this receptor does not solely promote the effects of FN1. Further studies may reveal how FN1 is regulated in imatinib-resistant cell lines and which players additionally contribute to the observed phenomenon.

Genome-wide methylation analyses showed a slight increase in overall methylation in imatinib and nilotinib resistance. In drug-resistant cancers, a variable extent of dysregulated methylation dependent on the drug and tumor was described, for instance 65% hypermethylated genes in patients with colorectal cancer undergoing 5-fluorouracil treatment or 44% hypermethylated genes in cisplatin-resistant lung adenocarcinoma A549 cells (41-43). For CML, it was revealed that DNA methylation increases moderately in blast crisis compared with chronic phase (44). In addition, it was demonstrated that the BCR-ABL1 fusion protein is able to alter DNA methylation, which can be reversed by imatinib or 5-azacytidine (45). Amabile *et al* (45) also found that only less than half of the differential methylated regions were associated with promoter regions in their CML tumorigenesis model consistent with observations of differential methylation in all genomic regions detected in the present study. It was identified that solely distinct genes were differentially methylated after TKI exposure or in TKI resistance, for instance *PTEN, PDLIM4, BIM, HOXA4, OSCP1* or *NPM2* (10,46-48). In the present study, hypermethylation of these genes was not detected, but *BCL2* (B-cell lymphoma 2), *PDE4DIP* (phosphodiesterase 4D interacting protein), *NMU* (neuromedin U), *IFI30* (gamma-interferon-inducible lysosomal thiol reductase) and *DNASE2* (deoxyribonuclease-2-alpha) were identified as candidate genes that were downregulated in imatinib resistance-potentially by DNA methylation in

their promoter region. With *BCL2*, *DNASE2* and *PDE4DIP*, three of five genes encode for regulators of apoptosis and cell cycle, it could be hypothsized that these genes are involved in the development of TKI resistance. However, further studies are necessary to reveal whether these genes and their DNA methylation are involved in the development of TKI resistance or could be used as potential prognostic biomarkers.

Studying drug resistance by using *in vitro*-cell lines is useful to identify mechanisms of resistance, to establish treatment protocols and to predict drug efficacy (49-51). The experiments are performed with cell lines derived almost exclusively as one single biological sample of a resistant cell line generated either by pulse treatment or continuous administration of increasing drug concentrations to the cells (52). For our *in vitro*-model, drug concentrations of 0.5 and 2 µM imatinib and 0.1 µM nilotinib were used to generate biological replicates of resistant sublines. The imatinib concentrations used depict the plasma levels measured in TKI-treated CML patients and reflect their high variation from 0.34 to 3 µM (53-55). A total of 0.1 µM nilotinib, however, was used to consider the 20-fold higher potency of nilotinib compared with imatinib (4). As *in vitro*-drug resistance models are generally only generated once, reproducibility is often lacking and therefore, transfer to the clinical situation is limited (51). Drug resistance models for CML were mainly obtained using a similar TKI concentration range and the same cell line model. However, large differences were observed, for instance shown for the influence of drug transporters in TKI resistance (56-59). This may be due to different TKI concentrations, cell line passages or clonal evolution occurring during the development of TKI resistance. Accordingly, biological replicates are essential to overcome this limitation and identify recurrent mechanisms of resistance. Therefore, biological replicates of TKI resistance were developed using the CML cell line K-562 to study recurrent mechanisms of resistance against imatinib and nilotinib. Although it was possible to identify alterations in cell adhesion signaling as potential recurrent mechanism of TKI resistance, the differences between the biological replicates indicated that genetic aberrations occurring during the development of resistance additionally contribute to this phenomenon.

In conclusion, studying TKI resistance *in vitro*, a TKI- and concentration-dependent change in genome-wide gene expression was observed. Further, a slight hypermethylation in TKI resistance was detected. However, the extent of gene and also methylation changes differed markedly between biological replicates demonstrating that biological replicates are crucial applying such models of acquired drug resistance. Notably, cell adhesion signaling, in particular the cellular matrix protein FN1, was found to be dysregulated in all resistant sublines. As proof of principle, experimental downregulation of FN1 led to a reduction of imatinib susceptibility indicating that FN1 may play a role in imatinib resistance and could potentially be used as a biomarker or target for future therapies.

Acknowledgements

for outstanding technical assistance, the Institute of Clinical Molecular Biology in Kiel for providing Sanger sequencing as supported in part by the DFG Clusters of Excellence 'Precision Medicine in Chronic Inflammation' and 'ROOTS' and Claudia Becher, Institute of Human Genetics, University Hospital Schleswig-Holstein, Kiel, for her technical assistance.

Availability of data and materials

Genome-wide gene expression (GSE203342, https://www.ncbi.nlm.nih.gov/geo/query/acc.cgi?acc=GSE203442) and methylation (GSE203443, https://www.ncbi.nlm.nih.gov/geo/query/acc.cgi?acc=GSE203443) datasets are available in the GEO repository. Further data generated and analyzed during this study are included in this published article and its supplementary information files.

Authors' contributions

MK and IN concepted the study and designed the research. MK, ML and JK performed the experiments. MK, ML, RB and OA analyzed the data. MK, HB and IN interpreted the data. MK, IC and IN wrote the manuscript. All authors read approved the final version of the manuscript. MK and IC confirm the authenticity of all the raw data.

Ethics approval and consent to participate

Not applicable.

Patient consent for publication

Not applicable.

Competing interests

The authors declare that they have no competing interests.

References

1. Deininger MW, Goldman JM and Melo JV: The molecular biology of chronic myeloid leukemia. Blood 96: 3343-3356, 2000.
2. Quintas-Cardama A and Cortes J: Molecular biology of bcr-abl1-positive chronic myeloid leukemia. Blood 113: 1619-1630, 2009.
3. Druker BJ, Tamura S, Buchdunger E, Ohno S, Segal GM, Fanning S, Zimmermann J and Lydon NB: Effects of a selective inhibitor of the Abl tyrosine kinase on the growth of Bcr-Abl positive cells. Nat Med 2: 561-566, 1996.
4. Baccarani M, Deininger MW, Rosti G, Hochhaus A, Soverini S, Apperley JF, Cervantes F, Clark RE, Cortes JE, Guilhot F, et al: European LeukemiaNet recommendations for the management of chronic myeloid leukemia: 2013. Blood 122: 872-884, 2013.
5. Hochhaus A, Larson RA, Guilhot F, Radich JP, Branford S, Hughes TP, Baccarani M, Deininger MW, Cervantes F, Fujihara S, et al: Long-term outcomes of imatinib treatment for chronic myeloid leukemia. N Engl J Med 376: 917-927, 2017.
6. Milojkovic D and Apperley J: Mechanisms of resistance to imatinib and second-generation tyrosine inhibitors in chronic myeloid leukemia. Clin Cancer Res 15: 7519-7527, 2009.
7. Soverini S, De Benedittis C, Papayannidis C, Paolini S, Venturi C, Iacobucci I, Luppi M, Bresciani P, Salvucci M, Russo D, et al: Drug resistance and BCR-ABL kinase domain mutations in Philadelphia chromosome-positive acute lymphoblastic leukemia from the imatinib to the second-generation tyrosine kinase inhibitor era: The main changes are in the type of mutations, but not in the frequency of mutation involvement. Cancer 120: 1002-1009, 2014.
8. Zabriskie MS, Eide CA, Tantravahi SK, Vellore NA, Estrada J, Nicolini FE, Khoury HJ, Larson RA, Konopleva M, Cortes JE, et al: BCR-ABL1 compound mutations combining key kinase domain positions confer clinical resistance to ponatinib in Ph chromosome-positive leukemia. Cancer Cell 26: 428-442, 2014.
9. de Lavallade H and Kizilors A: The importance of mutational analyses in chronic myeloid leukaemia for treatment choice. Eur Med J Oncol 4: 86-95, 2016.
10. Jelinek J, Gharibyan V, Estecio MR, Kondo K, He R, Chung W, Lu Y, Zhang N, Liang S, Kantarjian HM, et al: Aberrant DNA methylation is associated with disease progression, resistance to imatinib and shortened survival in chronic myelogenous leukemia. PLoS One 6: e22110, 2011.
11. Turrini E, Haenisch S, Laechelt S, Diewock T, Bruhn O and Cascorbi I: MicroRNA profiling in K-562 cells under imatinib treatment: Influence of miR-212 and miR-328 on ABCG2 expression. Pharmacogenet Genomics 22: 198-205, 2012.
12. Liu Y, Song Y, Ma W, Zheng W and Yin H: Decreased microRNA-30a levels are associated with enhanced ABL1 and BCR-ABL1 expression in chronic myeloid leukemia. Leuk Res 37: 349-356, 2013.
13. Shibuta T, Honda E, Shiotsu H, Tanaka Y, Vellasamy S, Shiratsuchi M and Umemura T: Imatinib induces demethylation of miR-203 gene: An epigenetic mechanism of anti-tumor effect of imatinib. Leuk Res 37: 1278-1286, 2013.
14. Cortes J and O'Dwyer ME: Clonal evolution in chronic myelogenous leukemia. Hematol Oncol Clin North Am 18: 671-684, 2004.
15. Corbin AS, Agarwal A, Loriaux M, Cortes J, Deininger MW and Druker BJ: Human chronic myeloid leukemia stem cells are insensitive to imatinib despite inhibition of BCR-ABL activity. J Clin Invest 121: 396-409, 2011.
16. Hamad A, Sahli Z, El Sabban M, Mouteirik M and Nasr R: Emerging therapeutic strategies for targeting chronic myeloid leukemia stem cells. Stem Cells Int 2013: 724360, 2013.
17. Kaehler M, Ruemenapp J, Gonnermann D, Nagel I, Bruhn O, Haenisch S, Ammerpohl O, Wesch D, Cascorbi I and Bruckmueller H: MicroRNA-212/ABCG2-axis contributes to development of imatinib-resistance in leukemic cells. Oncotarget 8: 92018-92031, 2017.
18. Oliveros JC: An interactive tool for comparing lists with Venn's diagrams. 2007-2015. https://bioinfogp.cnb.csic.es/tools/venny/index.html
19. Walter W, Sanchez-Cabo F and Ricote M: GOplot: An R package for visually combining expression data with functional analysis. Bioinformatics 31: 2912-2914, 2015.
20. RStudio Team (2020). RStudio: Integrated Development for R. RStudio, PBC, Boston, MA. http://www.rstudio.com/.
21. Pedregosa F, Varoquaux G, Gramfort A, Michel V and Thirion B: Scikit-learn: Machine learning in python. J Machine Learning Research 12: 2825-2830, 2011.
22. Kaehler M, Dworschak M, Rodin JP, Ruemenapp J, Vater I, Penas EMM, Liu C, Cascorbi I and Nagel I: Zfp36l1 plays an ambiguous role in the regulation of cell expansion and negatively regulates Cdkn1a in chronic myeloid leukemia cells. Exp Hematol 99: 54-64, 2021.
23. Waetzig V, Haeusgen W, Andres C, Frehse S, Reinecke K, Bruckmueller H, Ruwen Boehm H, Herdegen T and Cascorbi I: Retinoic acid-induced survival effects in SH-SY5Y neuroblastoma cells. J Cell Biochem 120: 5974-5986, 2019.
24. Bruhn O, Lindsay M, Wiebel F, Kaehler M, Nagel I, Böhm R, Röder C and Cascorbi I: Alternative polyadenylation of ABC transporters of the C-family (ABCC1, ABCC2, ABCC3) and implications on posttranscriptional Micro-RNA regulation. Mol Pharmacol 97: 112-122, 2020.
25. Edeki C: Comparative study of microarray and next generation sequencing technologies. IJCSMC 1: 15-20, 2012.
26. Pop L, Zanoaga O, Chiroi P, Nutu A, Korban SS, Stefan C, Irimie A and Berindan-Neagoe I: Microarrays and NGS for drug discovery. In: Drug Design. Parikesit AA (ed). IntechOpen, 2021.
27. Bakay M, Chen YW, Borup R, Zhao P, Nagaraju K and Hoffman EP: Sources of variability and effect of experimental approach on expression profiling data interpretation. BMC Bioinformatics 3: 4, 2002.

28. Bammler T, Beyer RP, Bhattacharya S, Boorman GA, Boyles A, Bradford BU, Bumgarner RE, Bushel PR, Chaturvedi K, Choi D, *et al*: Standardizing global gene expression analysis between laboratories and across platforms. Nat Methods 2: 351-356, 2005.

29. Draghici S, Khatri P, Eklund AC and Szallasi Z: Reliability and reproducibility issues in DNA microarray measurements. Trends Genet 22: 101-109, 2006.

30. Chung YJ, Kim TM, Kim DW, Namkoong H, Kim HK, Ha SA, Kim S, Shin SM, Kim JH, Lee YJ, *et al*: Gene expression signatures associated with the resistance to imatinib. Leukemia 20: 1542-1550, 2006.

31. Kim TM, Ha SA, Kim HK, Yoo J, Kim S, Yim SH, Jung SH, Kim DW, Chung YJ and Kim JW: Gene expression signatures associated with the in vitro resistance to two tyrosine kinase inhibitors nilotinib and imatinib. Blood Cancer J 1: e32, 2011.

32. Krause DS and Scadden DT: A hostel for the hostile: The bone marrow niche in hematologic neoplasms. Haematologica 100: 1376-1387, 2015.

33. Bazzoni G, Carlesso N, Griffin JD and Hemler ME: Bcr/Abl expression stimulates integrin function in hematopoietic cell lines. J Clin Invest 98: 521-528, 1996.

34. Nishihara T, Miura Y, Tohyama Y, Mizutani C, Hishita T, Ichiyama S, Uchiyama T and Tohyama K: Effects of the tyrosine kinase inhibitor imatinib mesylate on a Bcr-Abl-positive cell line: Suppression of autonomous cell growth but no effect on decreased adhesive property and morphological changes. Int J Hematol 78: 233-240, 2003.

35. Li Y, Clough N, Sun X, Yu W, Abbott BL, Hogan CJ and Dai Z: Bcr-Abl induces abnormal cytoskeleton remodeling, beta1 integrin clustering and increased cell adhesion to fibronectin through the Abl interactor 1 pathway. J Cell Sci 120: 1436-1446, 2007.

36. Windisch R, Pirschtat N, Kellner C, Chen-Wichmann L, Lausen J, Humpe A, Krause DS and Wichmann C: Oncogenic deregulation of cell adhesion molecules in leukemia. Cancers (Basel) 11: 311, 2019.

37. Damiano JS, Hazlehurst LA and Dalton WS: Cell adhesion-mediated drug resistance (CAM-DR) protects the K562 chronic myelogenous leukemia cell line from apoptosis induced by BCR/ABL inhibition cytotoxic drugs and gamma-irradiation. Leukemia 15: 1232-1239, 2001.

38. Obr A, Roselova P, Grebenova D and Kuželová K: Real-time analysis of imatinib- and dasatinib-induced effects on chronic myelogenous leukemia cell interaction with fibronectin. PLoS One 9: e107367, 2014.

39. Kumar R, Pereira RS, Zanetti C, Minciacchi VR, Merten M, Meister M, Niemann J, Dietz MS, Rüssel N, Schnütgen F, *et al*: Specific targetable interactions with the microenvironment influence imatinib-resistant chronic myeloid leukemia. Leukemia 34: 2087-2101, 2020.

40. Wlodek J and Pituch-Noworolska A: The influence of fibronectin on proliferation and apoptosis of acute lymphoblastic leukaemia cells in vitro. Pol J Pathol 69: 62-66, 2018.

41. Baharudin R, Ab Mutalib NS, Othman SN, Sagap I, Rose IM, Mokhtar NM and Jamal R: Identification of predictive DNA methylation biomarkers for chemotherapy response in colorectal cancer. Front Pharmacol 8: 47, 2017.

42. Guo R, Wu G, Li H, Qian P, Han J, Pan F, Li W, Li J and Ji F: Promoter methylation profiles between human lung adenocarcinoma multidrug resistant A549/cisplatin (A549/DDP) cells and its progenitor A549 cells. Biol Pharm Bull 36: 1310-1316, 2013.

43. Romero-Garcia S, Prado-Garcia H and Carlos-Reyes A: Role of DNA methylation in the resistance to therapy in solid tumors. Front Oncol 10: 1152, 2020.

44. Lebecque B, Bourgne C, Vidal V and Berger MG: DNA methylation and intra-clonal heterogeneity: The chronic myeloid leukemia model. Cancers (Basel) 13: 3587, 2021.

45. Amabile G, Di Ruscio A, Müller F, Welner RS, Yang H, Ebralidze AK, Zhang H, Levantini E, Qi L, Martinelli G, *et al*: Dissecting the role of aberrant DNA methylation in human leukaemia. Nat Commun 6: 7091, 2015.

46. Jose-Eneriz ES, Agirre X, Jimenez-Velasco A, Cordeu L, Martín V, Arqueros V, Gárate L, Fresquet V, Cervantes F, Martínez-Climent JA, *et al*: Epigenetic down-regulation of BIM expression is associated with reduced optimal responses to imatinib treatment in chronic myeloid leukaemia. Eur J Cancer 45: 1877-1889, 2009.

47. Elias MH, Baba AA, Husin A, Sulong S, Hassan R, Sim GA, Wahid SFA and Ankathil R: HOXA4 gene promoter hypermethylation as an epigenetic mechanism mediating resistance to imatinib mesylate in chronic myeloid leukemia patients. Biomed Res Int 2013: 129715, 2013.

48. Nishioka C, Ikezoe T, Yang J, Udaka K and Yokoyama A: Imatinib causes epigenetic alterations of PTEN gene via upregulation of DNA methyltransferases and polycomb group proteins. Blood Cancer J 1: e48, 2011.

49. Borisov N, Tkachev V, Suntsova M, Kovalchuk O, Zhavoronkov A, Muchnik I and Buzdin A: A method of gene expression data transfer from cell lines to cancer patients for machine-learning prediction of drug efficiency. Cell Cycle 17: 486-491, 2018.

50. Mirabelli P, Coppola L and Salvatore M: Cancer cell lines are useful model systems for medical research. Cancers 11: 1098, 2019.

51. Rumjanek VM, Vidal RS and Maia RC: Multidrug resistance in chronic myeloid leukaemia: How much can we learn from MDR-CML cell lines? Biosci Rep 33: e00081, 2013.

52. McDermott M, Eustace AJ, Busschots S, Breen L, Crown J, Clynes M, O'Donovan N and Stordal B: In vitro development of chemotherapy and targeted therapy drug-resistant cancer cell lines: A practical guide with case studies. Front Oncol 4: 40, 2014.

53. Peng B, Lloyd P and Schran H: Clinical pharmacokinetics of imatinib. Clin Pharmacokinet 44: 879-894, 2005.

54. de Kogel CE and Schellens JH: Imatinib. Oncologist 12: 1390-1394, 2007.

55. Picard S, Titier K, Etienne G, Teilhet E, Ducint D, Bernard MA, Lassalle R, Marit G, Reiffers J, Begaud B, *et al*: Trough imatinib plasma levels are associated with both cytogenetic and molecular responses to standard-dose imatinib in chronic myeloid leukemia. Blood 109: 3496-3499, 2007.

56. Gromicho M, Dinis J, Magalhães M, Fernandes AR, Tavares P, Laires A, Rueff J and Rodrigues AS: Development of imatinib and dasatinib resistance: dynamics of expression of drug transporters ABCB1, ABCC1, ABCG2, MVP, and SLC22A1. Leuk Lymphoma 52: 1980-1990, 2011.

57. Eadie LN, Hughes TP and White DL: ABCB1 overexpression is a key initiator of resistance to tyrosine kinase inhibitors in CML cell lines. PLoS One 11: e0161470, 2016.

58. de Lima LT, Vivona D, Bueno CT, Hirata RDC, Hirata MH, Luchessi AD, de Castro FA, de Lourdes F Chauffaille M, Zanichelli MA, Chiattone CS, *et al*: Reduced ABCG2 and increased SLC22A1 mRNA expression are associated with imatinib response in chronic myeloid leukemia. Med Oncol 31: 851, 2014.

59. Nies AT, Schaeffeler E, van der Kuip H, Cascorbi I, Bruhn O, Kneba M, Pott C, Hofmann U, Volk C, Hu S, *et al*: Cellular uptake of imatinib into leukemic cells is independent of human organic cation transporter 1 (OCT1). Clin Cancer Res 20: 985-994, 2014.